

QUANTITATIVE SUSCEPTIBILITY MAPPING AS AN IMPROVED BIOMARKER FOR CEREBRAL MICROBLEEDS IN SMALL VESSEL DISEASE

S. Beladi^{1,2}, C. R. McCreary^{1,2}, E. E. Smith^{1,3}, M. L. Lauzon^{1,2}, M. E. MacDonald¹, and R. Frayne^{1,2}

¹Seaman Family MR Centre, Foothills Medical Centre, Alberta Health services, Calgary, Alberta, Canada, ²Department of Radiology, University of Calgary, Calgary, Alberta, Canada, ³Department of Clinical Neurosciences, University of Calgary, Calgary, Alberta, Canada

INTRODUCTION

Cerebral microbleeds (CMBs) are hemosiderin deposits in the brain that surround small vessels and result from blood leaking through the vessel wall. CMBs have high prevalence in cerebral amyloid angiopathy (CAA), Alzheimer's disease (AD), stroke and small vessel disease (SVD). Emerging evidence shows that CMBs are clinically relevant markers of cognitive impairment and risk of brain hemorrhage [1,2]. Therefore, a method capable of imaging the CMBs with high sensitivity and spatial accuracy is of great importance. Imaging methods should be sensitive to sources that induce susceptibility changes. In T2*-weighted and susceptibility-weighted imaging (SWI), which are currently used for this purpose, CMBs are visualized as regions of signal voids. However, there are a number of limitations to these approaches: 1) non-local effects, 2) dependence on geometry and orientation of CMB relative to the main magnetic field [3], and 3) artifactual increase of signal void volume making accurate estimates of CMB size challenging [4]. Novel quantitative susceptibility mapping (QSM) [5] may overcome these limitations by accurately estimating the volume and quantity of susceptibility sources, such as iron (positive susceptibility) and calcium (negative susceptibility). Since CMBs contain iron (hemosiderin), we hypothesize that QSM can improve CMB detection and potentially provide an enhanced biomarker for SVD. Here, QSM and SWI are compared in CAA patients to better visualize CMBs, estimate CMB volume, and generate susceptibility maps that are independent of the imaging parameters.

METHOD

Five CAA patients, diagnosed according to the validated Boston criteria, were imaged on a 3 T scanner (Signa VH/i; GE Healthcare, Waukesha, WI), with an 8-channel head coil. A 3D single-echo gradient-recalled-echo (GRE) sequence was used with the following imaging parameters: TE = 20 ms, TR = 30 ms, voxel size = 0.47 mm × 0.47 mm × 2 mm, acquired matrix size = 512 × 256 × 60 (interpolated to 512 × 512 × 120). Images were down sampled in the slice direction to improve calculation speed for QSM. Phase images were unwrapped using a magnitude-guided algorithm [6]. The field changes reflected in the unwrapped phase map were generated by the local magnetic sources (such as CMBs) and also by the variations in the magnetic susceptibility in surrounding area (such as at air-tissue interfaces). It is necessary to first remove the background field from the unwrapped phase image using effective dipole-fitting [7]. Because the forward problem in QSM is ill-conditioned, the susceptibility maps were estimated by solving an optimization problem. As the distribution of CMBs is sparse in the brain, we used L1-norm optimization to promote sparsity.

The optimization is given by $\min \|C\chi - \varphi\|_2 + \lambda \|\chi\|_1$, where χ , C are the susceptibility map and the convolution matrix (representing the convolution by the unit dipole field), respectively. Also, φ and λ represent the normalized field-shift and the regularization parameter, respectively. The resulting matrix sizes are extremely large and as a result the matrices were not explicitly formed. The inverse problem was solved using the iterative log-barrier numerical method [8]. A stroke neurologist identified the CMBs on the SWI images, a CMB mask was created, and the mask was compared with the QSM map in 80 randomly selected regions of interest (ROIs) over the subjects. Each ROI included a CMB and some surrounding tissue. The volumes of individual CMBs were determined for both SWI and QSM. The student's *t*-test was used to examine the differences in signal values of CMB and the surrounding tissue.

RESULTS

The average signal change in SWI (CMB compared to surrounding tissue) was -33%, while the average signal difference in QSM was +170% ($p < 0.01$). The total CMB volume in SWI and QSM were 482.4 mm³ and 282.3 mm³, respectively. The CMB volume on SWI was on average 1.7 times larger ($p < 0.01$). Fig 1 shows the CMB volume distribution. The majority of CMBs on SWI had volumes <8 mm³. SWI showed some CMBs with volumes >24 mm³. Fig 2 illustrates one case where three adjacent CMBs that were not well discriminated on SWI were clearly visualized on QSM. By removing blurring effects, QSM improved visualization of small, adjacent CMBs.

DISCUSSION

This study evaluated the diagnostic values of SWI and QSM for detecting CMBs in patients with CAA. We found that SWI overestimated the QSM CMB volume by 170% due to the blooming effect. QSM also solves the problem of non-local effects and provides more accurate maps. The mean volume of individual CMBs was reported as 3.5 mm³ and 6.0 mm³ for QSM and SWI, respectively. The number of CMBs with volumes more than 13.2 mm³ in SWI was 2 times larger than in QSM. Also, the magnitude of the relative signal change between the CMB and the surrounding normal tissue was significantly higher in QSM (+170%) compared to SWI (-30%). In addition, QSM has the ability to discriminate between tiny adjacent CMBs that are presented as a single large CMB in SWI.

CONCLUSION

Application of QSM to CAA patients showed that CMB detection can be improved compared to the results obtained from SWI. QSM removes the problems of non-local effects and over-sized CMBs, and provides quantitative values that are independent of the imaging parameters. Future studies will focus on removing artifacts in the QSM maps, evaluation of results for different regularization parameter values, and quantification of CMBs in patient groups.

REFERENCES

- [1] Werring *et al.*, *Neurology*. 2005; 65: 1914-8.
- [2] Cordonnier *et al.*, *Brain*. 2011; 134: 3335-44.
- [3] Schafer *et al.*, *Neuroimage*. 2009; 48:126-37.
- [4] Schrag *et al.*, *Acta Neuropathol*. 2010; 119:291-302.
- [5] De Rochefort *et al.*, *Magn Reson Med* 2010; 63: 194-206.
- [6] Jenkinson *et al.*, *Magn Reson Med* 2003; 49(1): 193-197.
- [7] Liu *et al.*, *Proceeding of ISMRM* 2010; p 141.
- [8] Boyd *et al.*, *Convex Optimization*, Cambridge, U.K, 2004.

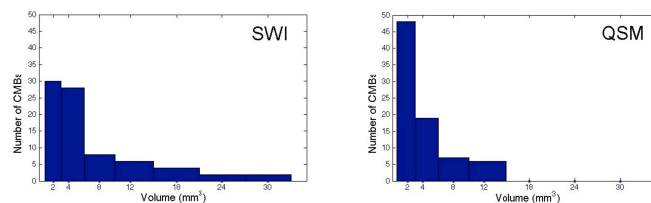


Figure 1: CMB volume histograms for SWI (left) and QSM (right).

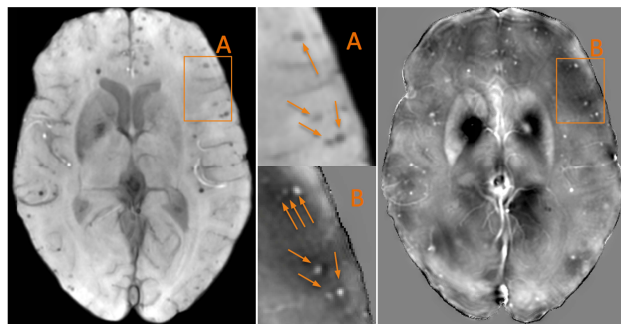


Figure 2: SWI (left) and QSM (right) for demonstrating CMBs. As shown in A and B, QSM discriminates small adjacent CMBs (arrows).